jove

Microfabrication of Implantable Optics Integrated in a Microstructured Imaging Window for Advanced *In Vivo* Imaging

Alessandra Nardini[1,2,3], **Behjat Sadat Kariman**[4], **Mario Marini**[5], **Claudio Conci**[1], **Marco Grassi**[1], **Margaux Bouzin**[5], **Maddalena Collini**[5], **Roberto Osellame**[2], **Giulio Cerullo**[4], **Manuela Teresa Raimondi**[1], **Giuseppe Chirico**[5], **Rebeca Martínez Vázquez**[2]

[1] Department of Chemistry, Materials and Chemical Engineering "Giulio Natta", Politecnico di Milano [2] Istituto di Fotonica e Nanotecnologie (IFN), Consiglio Nazionale delle Ricerche (CNR) [3] Department of Experimental Medicine, Università del Salento [4] Department of Physics, Politecnico di Milano [5] Department of Physics, Università di Milano-Bicocca

Corresponding Author

Rebeca Martínez Vázquez
rebeca.martinezvazquez@cnr.it

Citation

Nardini, A., Kariman, B.S., Marini, M., Conci, C., Grassi, M., Bouzin, M., Collini, M., Osellame, R., Cerullo, G., Raimondi, M.T., Chirico, G., Martínez Vázquez, R. Microfabrication of Implantable Optics Integrated in a Microstructured Imaging Window for Advanced *In Vivo* Imaging. *J. Vis. Exp.* (218), e67975, doi:10.3791/67975 (2025).

Date Published

April 11, 2025

DOI

10.3791/67975

URL

jove.com/video/67975

Abstract

In the context of biomaterials and drug testing in animal models, this study presents a streamlined protocol for fabricating a novel implantable integrated imaging window. The micro-device comprises a sophisticated system of microlenses coupled with micro-scaffolds specifically designed for *in vivo* quantification of the immune response using advanced non-linear excitation microscopy. The protocol is based on two-photon polymerization (2PP) of the biocompatible photoresist SZ2080, which enables the fabrication of micro-scaffolds and micro-lenses in a continuous sequence to enhance manufacturing efficiency and precision. To further improve speed, accuracy, and structural integrity, a hybrid optics fabrication approach was implemented, involving the 2PP of the microlens outer shell followed by UV bulk crosslinking of the inner core. This innovative technique optimizes the optical properties of the microlenses while streamlining the production process. The resulting micro-device demonstrates high reproducibility and mechanical stability, making it an effective method for prototyping microscale optical systems for a range of biomedical applications.

Introduction

Intravital microscopy empowers the study of biological processes in living animals by real-time visualization. When combined with fluorescent non-linear imaging approaches, it can even reach a resolution at the sub-cellular scale[1]. Consequently, it has become an important tool in many fields, such as immunology tests or cancer studies, where

observation of the cells inside their real physiological environment is important.

Common approaches for intravital inspections, such as dorsal skinfold chambers or cranial and abdominal imaging windows, are highly invasive and pose difficulties for long-time inspections of the same point. Thus, new *in vivo* imaging approaches that reduce animal distress and allow easy repositioning of the optical view are strongly desirable[2].

In this framework, it is possible to advance a novel miniaturized imaging window based on a glass substrate that contains an imaging side with optical microlenses and a tissue reference side with three-dimensional (3D) micro-scaffolds. This miniaturized imaging window can be implanted "subcute" in the animal and will function as an "internal" microscope objective. The device work principle will be to use the microlenses coupled with an external low Numerical Aperture (NA) microscope objective to perform *in vivo* non-linear imaging of the biological processes taking place inside the scaffolds. The microlenses will compensate for spherical aberration due to imaging through an inhomogeneous media as tissue[3,4], while the micro-scaffold will drive tissue regeneration and will act as optical beacons[5,6,7], thus permitting the long-time inspection of the same point.

The basic components of the device, i.e., micro-scaffolds and micro-lenses, have already been demonstrated separately, but their integration in the same device presents several challenges due to their 3D nature, their micrometer size, and the need to have a perfect optical alignment between them. The micro-scaffolds, consisting of rectangular cuboid grids, with representative overall dimensions ~ 500 µm x 500 µm x 100 µm and with pore sizes ~ 50 µm x 50 µm x 20 µm, can guide cell recruitment and new vascularization, thus promoting tissue integration. Furthermore, due to their autofluorescence, the micro scaffolds function as an *in situ* fluorescence beacon thus allowing a fast repositioning and alignment under the microscope and even a correction of spherical aberrations during non-linear imaging to enable high-resolution longitudinal *in-vivo* observations[5]. The high-numerical aperture microlenses, with spherical or quasi-parabolic profiles and focal lengths of a few hundred micrometers, have demonstrated their capabilities for linear and non-linear imaging of biological specimens if combined with a confocal or two-photon microscope[3,4].

The microlenses and the micro-scaffolds are fabricated by 3D laser inscription, also known as two-photon polymerization (2PP). In 2PP, an infrared femtosecond laser beam is tightly focused inside a UV curable photoresist, and due to multi-photon absorption at the focal spot, a confined voxel of polymerized material is created with sub-micrometer size (~100 nm). By moving the laser focus with respect to the photoresist sample, three-dimensional structures of polymerized material can be obtained after washing away the un-polymerized material[8]. The process has an intrinsically high resolution and a 3D nature that allows the acquisition of 3D microstructures, like scaffolds and lenses, with good stability and high surface quality[9,10,11]. There are different techniques for the fabrication of porous micro-scaffolds like 3D printing, nanoimprinting, or electrospinning[12,13,14,15]. All these techniques suffer from a main drawback; they are not able to reach resolutions in the sub-micrometer range, thus giving structures with pores sizes (~100 µm) larger than the cellular size, and do not mimic extracellular matrix, which is essential for good tissue regeneration. The fabrication of microlenses can be approached by methods based on the replication of the lens from a mold or mask like injection molding, hot embossing, or UV molding, or by direct methods like thermal reflow, microplastic embossing or microdroplet jetting[16,17]. All of them present limitations on surface morphology that can be obtained and are

difficult to integrate into a fabrication flow where the micro-scaffolds must also be manufactured. On the other side, 2PP has demonstrated its versatility for the fabrication of complex optical components[18,19], like spheric or parabolic lenses, diffractive lenses, or even combinations of different lenses in the same optical component[20,21,22,23,24]. In this framework, 2PP appears to be the best technique for the fabrication of a whole that contains both lenses and micro-scaffolds.

Despite being a unique choice for the realization of these 3D structures with micrometer resolution, 2PP presents two main limitations, i.e., it is a time-consuming approach for relatively large volume structures, and it presents a limited fabrication depth (along the optical axis) due to the short working distance of microscope objectives used for tight focusing.

This article proposes a unique protocol for the fabrication of the micro-scaffolds and the microlenses on the opposite sides of a glass substrate in a one-longitudinal step irradiation process that guarantees a good alignment of both elements and overcomes the limitations of fabrication depth. The protocol is also optimized for fabrication time; on the one hand, the one-step irradiation saves alignment time, and the use of a hybrid approach that combines 2PP of the lens shell and UV curing of the inner photoresists reduces irradiation time for the high-volume lenses[25]. The ability of 2PP to fabricate free-form 3D structures permits the use of this protocol for any microlens and micro-scaffold design, thus empowering the current method.

Protocol

The details of the reagents and the equipment used in this study are listed in the **Table of Materials**.

1. Sample preparation

1. First drop-casting (**Figure 1A**)
    1. Clean with acetone on both surfaces of a 12 mm diameter circular glass coverslip (170 µm thickness).
    2. Dry both surfaces with room-temperature Nitrogen gas.
    3. Deposit a controlled amount of 46 µL of liquid photoresist on one side of the glass coverslip using a volume pipette.

        NOTE: The photosensitive material used in this protocol is a biocompatible, hybrid organic/inorganic photoresist known as SZ2080, which is well-known and validated for biomedical applications[26]. Pay attention to leave a free external annulus on the glass substrate. Being free of photoresist, this glassy space ensures the correct holding of the sample inside the support to better assist the preparation.
    4. Leave the sample under the chemical hood for 48 h to allow the drying of the first drop of photoresist by the evaporation of the solvent, reaching the sol-gel state.
2. Second drop-casting (**Figure 1A**)
    1. When the first drop of photoresist reaches the sol-gel state (step 1.1.4.), flip the sample upside down, exposing the clean surface.
    2. Place the sample on a supporting holder, lifting the first drop-casted surface from the ground.
    3. Deposit a second drop of 46 µL of liquid photoresist on the clean glass surface, leaving the external annulus as well as in step 1.1.3.

4. Leave the sample under the chemical hood for at least 48 h, letting the solvent to evaporate.

   NOTE: After 4-6 days, the double drop-casted sample is ready to be used for 2PP (**Figure 1B**). From now on, pay attention to not exposing the sample to ambient light due to the photosensitive material. Light exposure degrades the photoresist.

2. Two-photon polymerization (2PP) of the microstructures

1. Setup alignment (**Figure 2**)

   1. Switch on the femtosecond near-infrared laser source (1030 nm wavelength, 1 MHz, with minimum pulse duration = 230 fs).

      NOTE: Set laser parameters like the pulse width and the repetition rate.

   2. Align the laser beam's optical path until it reaches the microscope objective through a series of optics and mirrors mounted on kinematic mirror mounts. Iteratively rotate the mirrors to center the beam within near-infrared (NIR) alignment pinholes.

      NOTE: The microscope objective working distance should be longer than the total height of the final device to be manufactured (lens height + coverslip thickness + micro-scaffold height). NIR pinholes are properly designed to simplify the alignment of IR beams. This ensures precise beam alignment along the optical pathway, passing through components such as a half-wave plate, a beam expander, and a dichroic mirror. To automatically control the laser power, the beam passes through a horizontal polarizer and half-wave plate, and the second is mounted on a motorized rotator. If needed, the beam can pass through a beam expander to enlarge the beam diameter and fulfill the objective back entrance.

   3. Direct the laser beam perpendicularly to the sample holder by aligning it using back-reflection centering.

   4. Mount the long working distance microscope objective on the dedicated support at the end of the optical path close to the sample (**Figure 2**).

      NOTE: A CCD camera is mounted above the dichroic mirror aligned to the objective optical axis for fabrication process monitoring. It will allow one to see the laser focus spot and the polymerized structures.

2. Sample mounting

   1. Fix (with tape) the double-dropped glass coverslip on the sample holder mounted on the translation stages. Mount the sample with the second deposited drop facing down.

      NOTE: The sample holder has a central hole where the sample can be suspended from the ground stage[5]. The holder is connected to a gimbal mechanical system that is screwed to a X, Y translational stage for sample motion.

   2. Center the sample manually with the mounted microscope objective.

3. Sample centering

   1. Set the laser power at the minimum value sufficient to see the beam reflection on the CCD camera software (around 5 mW).

      NOTE: Measure the laser power at the back pupil of the objective (the transmission of the objective used in this protocol is 70% at 1030 nm wavelength.)

2. Switch on the operator interface software for the motion controller and the CCD camera.
3. Focus the laser beam on the upper surface of the first photoresist drop.
4. Following the curved profile of the drop, find the sample edges along the X and Y directions. Set the center of the drop as an absolute zero reference by software.
   NOTE: The tape used to fix the sample plays a role in the detection of edges by modifying the refractive index, hence beam reflection.

4. Sample tilt compensation
   1. In the center of the sample, focus the laser beam on the interface surface between the upper surface of the glass coverslip and the base of the first drop of photoresist. Set it as zero reference on the Z axis.
   2. Considering the diameter of the sample, move to the edge position (for the 12 mm coverslip, it is ~ - 4 mm) in the negative direction of the X-axis. In that position, focus the interface surface (between the glass and the upper drop of photoresist) and set it as an absolute zero reference along the vertical direction Z.
   3. Move to the edge position in the positive direction of the X axis (for the 12 mm coverslip, it is ~ + 4 mm). Find here the interface surface moving the objective along the vertical direction Z.
   4. Tilt the sample to correct for the deviation in the Z direction between the negative and positive positions along the X axis. Use an adjustable kinematic mounting for sample-holder tilting (like a gimbal).
   5. Repeat steps 2.4.2-2.4.4 iteratively until the sample is completely balanced on the X-axis.
   6. Perform the same procedure described in steps 2.4.2-2.4.5 along the Y direction.
   7. Once the sample is perfectly balanced on both the X and Y planar axis, come back to the central position and focus the interface between the glass and the photoresist at that point.
   8. Set the new Z value of the focus as a reference in the Z axis (Z = 0).
      NOTE: The procedure in step 2.4 is aimed at ensuring the perfect perpendicularity between the laser beam and the coverslip surface to ensure a perfect anchoring of the 2PP structures that will be fabricated later. From 2.4 on, all the procedures must be performed matching the refractive index. Therefore, add the objective's medium of index matching if needed.

5. Micro-scaffolds 2PP on the lower photoresist drop
   1. Switch on a red LED illumination system for real-time monitoring of the polymerization process.
      NOTE: A red-light emitting diode illumination is placed under the complex sample holder-gimbal (**Figure 2**). This illumination will allow one to see the polymerized volume during the 2PP process. The photoresist is sensitive to shorter wavelengths (visible light); therefore, the red-LED light is not going to perturb the sample.
   2. With the laser off, move the objective along the Z direction below the glass coverslip to find the second interface surface between the bottom surface of the glass and the base of the lower drop of resist.

NOTE: The second interface will be found at a Z value approximately equal to the coverslip thickness (170 µm).

3. Increase the laser power up to 100 mW to let two-photon polymerization occur in the bottom drop.

4. Tune the focal position (increasing Z) to find the second interface by polymerizing a simple reference structure.
   NOTE: An example of a reference structure is a 50 µm length polymerized line.

5. Set the first focal position where the polymerization of the reference structure takes place as the zero reference along the vertical direction (Z axis).
   NOTE: The reference in step 2.5.5 underlines the base plane for the 2PP of the micro-scaffolds.

6. Set the polymerization powers (~ 100-200 mW) and run the machine code as a computer numerical control (CNC) program for the proper motion of the translational stages to fabricate the desired 3D structure (**Figure 3A**).
   NOTE: The CNC program is made up of a set of spatial coordinates (x, y, z) that determine which way the translational platforms move to produce the final 3D object. These polymerization powers will be influenced by the height of the upper drop and the specific experimental conditions (photoresist, laser, and movement system).

6. Microlenses 2PP on the upper photoresist drop

1. Moving along the Z axis, come back to the first interface between the upper glass surface and the upper drop of photoresist (step 2.4.8). Maintain the same planar reference system (X, Y coordinate) to ensure a perfect alignment of the microlenses 2PP with the already fabricated microstructures.

2. Find the interface by polymerizing a simple reference structure.
   NOTE: Use the same process described in step 2.5.4, but only differing in the direction of the vertical motion.

3. Set the first line of polymerization as zero reference along the vertical direction (Z axis).
   NOTE: The reference in step 2.6.3 underlines the ground plane for the 2PP of the microlenses.

4. Set the fabrication parameters for the 2PP of the contour of the desired microlens (**Figure 3B**). The laser beam describes a circular trajectory decreasing in radius to continuously polymerize the external surface of a single microlens. Set the hatching and slicing parameters along the X and Z directions, respectively.
   NOTE: The design of the lenses should consider the effective focal length desired by the user. As a rule of thumb, it should be a value longer than the coverslip thickness, and it should allow to image the whole atlas. A preliminary computational simulation of the final optical system is recommended.

5. Set the polymerization power (~ 15-20 mW) and run the program that guides the motion of the translational stages.
   NOTE: These polymerization powers will be influenced by the height of the upper drop, the specific experimental conditions, and the design of the desired microlens (**Figure 3B**). **Figure 4** displays a representative example of parabolic microlens with

the parametric function that describes the microlens profile and its main geometrical features.

3. Sample development

1. Remove the sample from the experimental fabrication setup.
    1. With the laser off, disable the X, Y, and Z translational axis and remove the holder.
    2. Peel off the sticky tape and detach the sample from the holder.
    NOTE: Prior to sample development, pay attention to not exposing the sample to ambient light due to the photosensitive material. Light exposure would crosslink the whole amount of photoresist.
2. Sample development (**Figure 5A**)
    1. Place the sample in a proper support to lift it from the ground and hold it in a horizontal position.
    NOTE: This sample holder is a custom SLA-printed sample rack properly designed to expose both the 2PP prototyped surfaces to the developing solution[5].
    2. Prepare a 50 mL beaker and place the support carrying the sample inside it.
    NOTE: Pay attention to maintaining the 2PP microlenses on the upper surface to avoid any structural deformation during development due to their unpolymerized inner core.
    3. Fill the beaker with ~20 mL of developing solution, completely covering the sample. The solution is made by 50% (v/v) 2-pentanone and 50% (v/v) isopropyl alcohol solution.
    4. Leave the sample inside the developing solution for 45 min.
3. Sample washing
    1. Lift the support from the developing solution.
    2. By manually handling it or by using a pair of tweezers, take the sample and wash it carefully with a few drops of isopropyl alcohol.
    3. Dry both the fabricated surfaces of the glass coverslip with a gentle flow of Nitrogen (at room temperature).
    NOTE: All the procedures described in steps 3.2-3.3 are performed under a chemical fume hood.

4. Sample UV irradiation

1. Microlense exposure to UV radiation (385 nm wavelength) (**Figure 5B**)
    1. Place the glass coverslip on a sample holder suspended from the ground plane. Lay the sample with the microlenses facing down.
    NOTE: The sample holder has a central hole to place the sample suspended from the ground stage, preserving microstructure integrity on the bottom surface.
    2. Prepare a UV lamp with a wavelength of 385 nm.
    3. Position the sample under the UV source perpendicularly oriented with respect to the surface of the glass coverslip.
    4. Expose the sample to UV radiation set at 300 mW for 120 s.
    NOTE: The UV exposure occurs passing through the micro-scaffold and glass substrate. In this way, the not yet polymerized core of the lenses will be UV

crosslinked, avoiding direct and additional exposure to the previously polymerized surface.

5. Titling the UV source at -45° and +45° with respect to the normal position of the sample plane, repeat step 4.1.4.

   NOTE: This three-step UV exposure at different angles will allow for fully crosslinking the entire unpolymerized resist within the microlenses volume, achieving stability. This is particularly important for wide microlenses.

6. Remove the sample from the holder and store it.

5. Morphological characterization

1. Scanning Electron Microscopy (SEM) acquisitions (**Figure 6**)
   1. Prepare the SEM station. Attach a piece of carbon tape to the SEM holder for sample adherence.
   2. Place the glass sample on the holder at 45° with respect to the orientation of the SEM camera. Pay attention to attaching the sample in an empty space on the coverslip to preserve structure integrity (**Figure 6B**).
   3. Repeat the acquisition as in step 5.1.2 for both the surfaces of the glass coverslip to collect 3D SEM images of the micro-scaffolds and the microlenses (**Figure 6A,C**).
   4. Carefully detach the sample from the carbon tape and store it in a covered box.

Representative Results

A protocol for the fabrication of a double-sided implantable microstructured device containing an optical system and a tissue analysis reference has been provided. The process exploits two-photon laser polymerization to fabricate 3D microstructures and micro-optics on the opposite side of the same substrate. The use of a long working distance objective permits the fabrication of both structures without flipping the substrate, saving the re-alignment step and warranting a perfect alignment between both components. This device will empower advanced imaging *in situ* by allowing optical aberrations correction and repeated observations of the same area, thanks to micro-optics and a microfabricated frame of reference. **Figure 1** shows the procedure for preparing both surfaces of the supporting substrate for subsequent manufacturing. A sketch of the experimental setup used to microfabricate both surfaces of the sample is represented in **Figure 2**. The image also shows the complex objective-sample holder, with the first focusing on the sample that is illuminated by a red-LED illumination system, allowing real-time monitoring of the manufacturing using machine vision. **Figure 3** qualitatively demonstrates the protocol's flexibility in allowing the microfabrication of various designs of micro-scaffolds and microlens. **Figure 4** highlights the sag function used to design microlens with an aspheric parabolic profile and a sketch of a representative design correlated to its main features as an example. In **Figure 5**, the sample development and UV exposure steps necessary to crosslink the whole volume of the microlenses fully are reported. Finally, **Figure 6** shows examples of microfabrication outcomes. The presented procedure allows for the polymerization of 3D micro-structures of both surfaces of the same device, ensuring excellent resolution and stability. Lastly, **Figure 7** is an illustration representing the general workflow of the protocol, ending with **Figure 8**, which shows an example of a final application of the proposed device, i.e., *in vitro* imaging of cells grown inside the micro-scaffold.

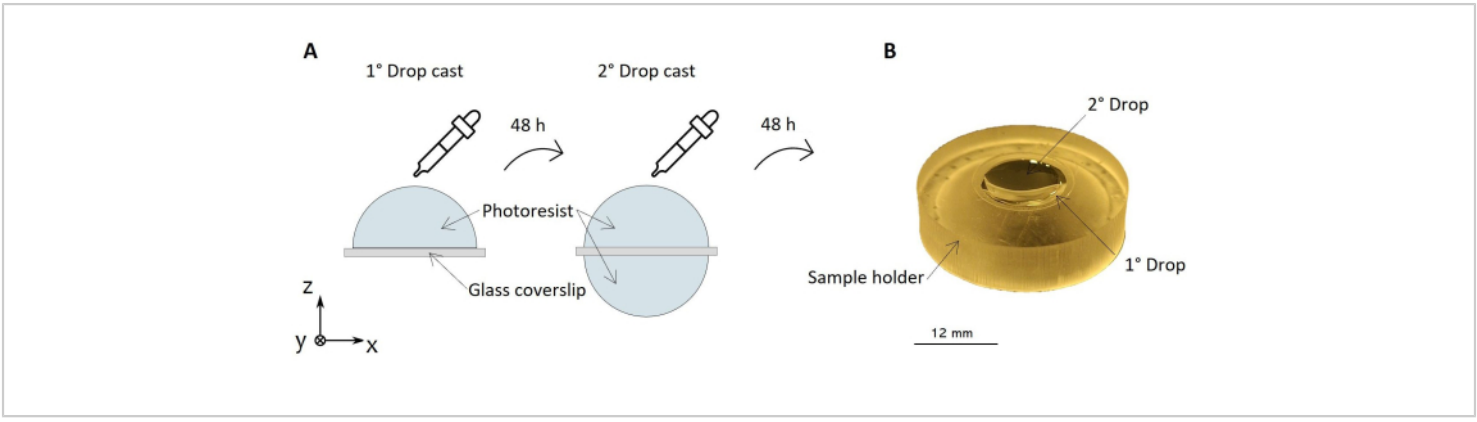

Figure 1: Protocol for sample preparation. This image shows a sketch of the double-step process for photoresist drop-casting on a supporting circular glass coverslip (**A**). On the right, a picture of the sample with the dried photoresist deposited on both sides is reported (**B**). The sample is supported by the sample holder. Please click here to view a larger version of this figure.

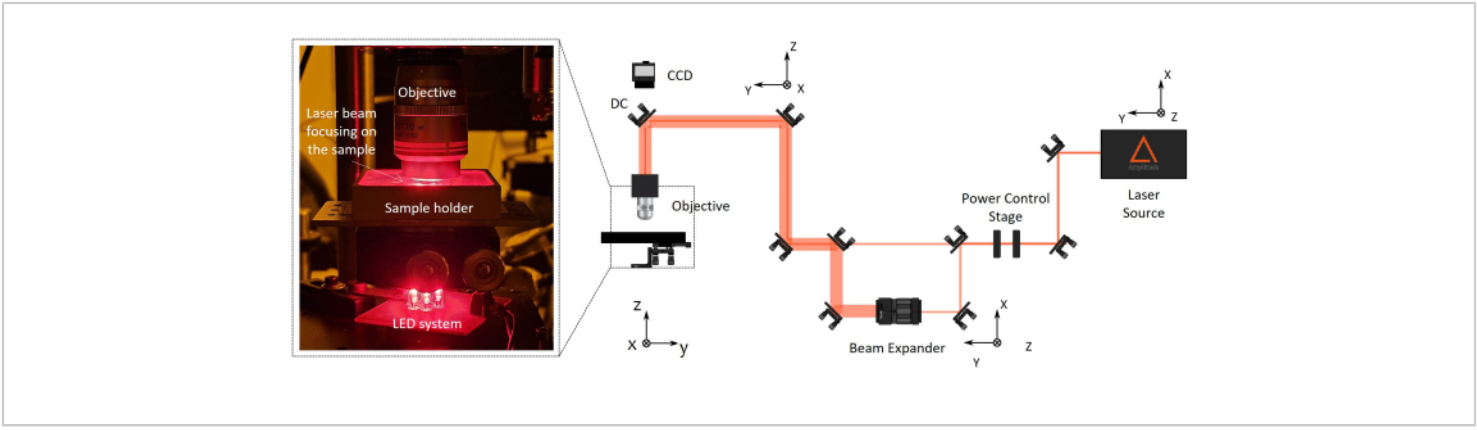

Figure 2: Two-photon laser polymerization (2PP) fabrication setup. On the right, a representative diagram of the fabrication setup is reported. The setup main components are a femtosecond laser source with a wavelength of 1030 nm, min pulse width of 230 fs, and 1 MHz repetition rate), a stage for power control, a beam expander, a dichroic mirror, and a high numerical aperture microscope objective (100x, NA 1.1). A CCD camera is mounted above the dichroic mirror aligned to the objective optical axis for fabrication process monitoring. On the left, there is a blow-up, with the zoom of the final part of the optical setup showing a photograph of the complex objective/sample-holder/LED illumination system for machine vision. Please click here to view a larger version of this figure.

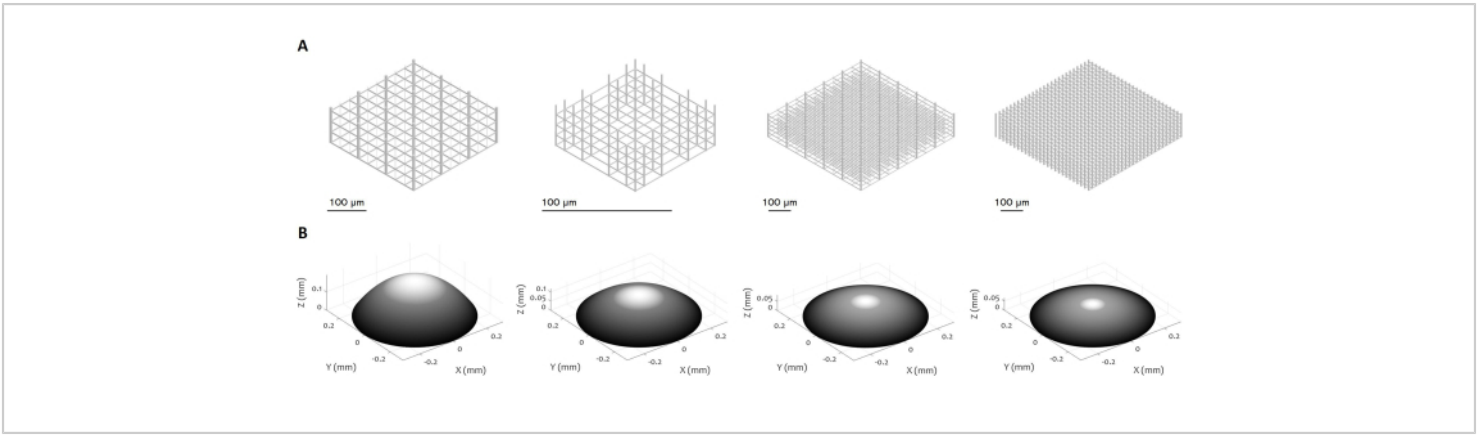

Figure 3: Multiple designs of 3D microstructures and microlenses. The figure displays various examples of (**A**) micro-scaffolds and (**B**) microlenses that can be manufactured using the proposed procedure. The high flexibility of the protocol enables the fabrication of microstructures with a variety of geometrical features, resolution, dimensions, and volume, demonstrating its versatility. The grey scale in panel (**B**) aims to highlight the decrease in laser power and writing speed to smooth the surface and minimize the surface roughness. Precise parameters of fabrication are set according to the specific design of the microlens. Scale bars: 100 µm. Please click here to view a larger version of this figure.

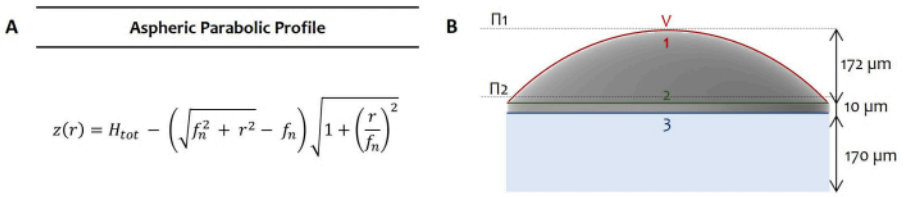

C

Surface	Thickness [µm]	Material	Refractive Index [λ 800 nm]	Radius [µm]	Effective Focal Length [µm]
1	172	SZ2080	1.46	300	
2	10	SZ2080	1.46	300	342 ± 10 µm
3	170	N-BK7	1.52	300	

Figure 4: Example of fabricated microlens. The panel shows a representative example of an aspheric parabolic profile highlighting the parametric description of the lens's curved surface as sag function z(r) (**A**). Here, H_{tot} is the lens thickness, r is the radial coordinate, and f_n is the focal length of a parabolic refractive lens that differs from its effective focal length. The dioptric power is determined by the lens's refractive index and how it differs from the ones of the surrounding medium. On the right, the design sketch highlights the two principal planes lying at the vertex V1 and a few µm above surface 2 (Π1 and Π2, dashed lines) (**B**). The sketch shows a single aspheric parabolic microlens with a diameter of 600 µm and fabricated on an N-BK7 glass substrate (with a thickness of 170 µm). (**C**) underlines the geometrical parameters for the aspheric parabolic lens microfabricated in SZ2080 photoresist. Please click here to view a larger version of this figure.

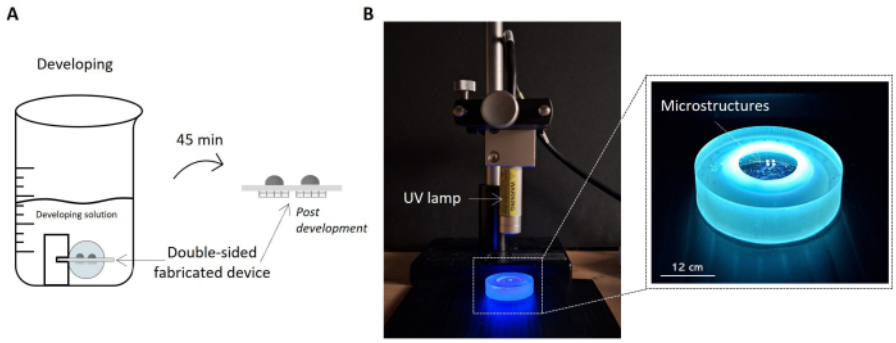

Figure 5: Protocols for sample development and UV exposure. The image highlights the fabricated sample soaked in the development solution as a sketch (**A**). The sample is lifted inside the solution by the holder, allowing the proper development of both sides of the sample and obtaining the double-sided microstructured device. On the right, a picture of the setup configuration for UV irradiation of the sample is reported (**B**). The picture shows the UV lamp positioned perpendicular to the surface of the sample. As stated in the UV lamp's datasheet, the current distance between the lamp and the sample is consistent with the lamp's operating distance. The sample undergoing UV radiation and handled by the sample holder is highlighted in the zoom-in image on the right. Scale bar: 12 cm. Please click here to view a larger version of this figure.

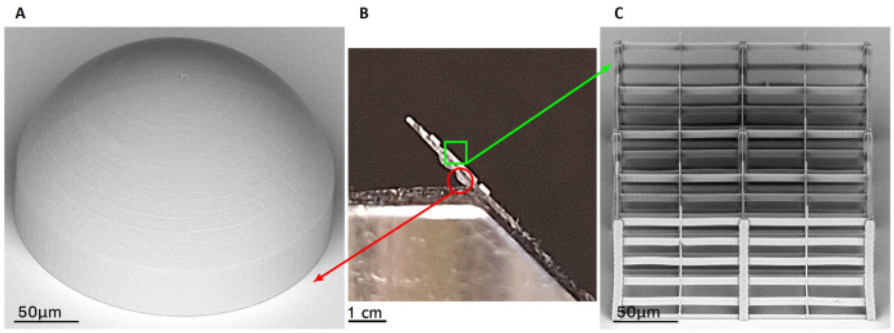

Figure 6: Scanning electron microscopy (SEM) acquisitions of representative outcomes of fabrication. The panel highlights a double-sided fabricated device through a lateral view (**B**) and two representative results of fabricated microlens (**A**) and micro-scaffold (**C**) by SEM images. The two constructs laying on different faces of the same glass substrate are clearly visible in the central picture (**B**). The microlenses are represented on the bottom surface of the glass, while the micro-scaffolds are on the upper one. The SEM image of fabricated microlens with a spheric design is shown on the right as an example of the stable and smooth outcome of fabrication (**A**). On the left, the image highlights a representative result of a 2PP porous micro-scaffold with arbitrary geometry (**C**). Scale bars: (**A,C**) - 50 µm; (**B**) - 1 cm. Please click here to view a larger version of this figure.

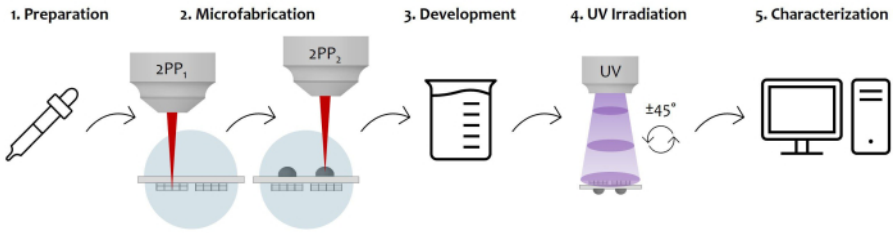

Figure 7: Schematic diagram of the protocol workflow and device application: The figure displays the overall manufacturing process sketched step by step. It starts with the preparation of the sample by the sequential photoresist drop-casting on both surfaces of the glass substrate (1). Once the photoresist reaches a sol-gel state, the sample is ready to be fabricated by two-photon laser polymerization (2). Therefore, both the photoresist drops are sequentially irradiated, microstructuring the microstructures first and then the microlenses. Afterward, the double-sided microfabricated substrate undergoes a developing procedure to remove all the unpolymerized resist surrounding the constructs (3). To do so, the sample is soaked in an alcoholic solution and then gently dried. Follows the UV irradiation of the sample by passing through the glassy substrate to completely crosslink the unpolymerized inner core of the microlenses (4). Lastly, a quality check of the microfabricated sample is performed by Scanning Electron Microscopy (SEM) acquisitions to morphologically characterize the microstructures (5). Please click here to view a larger version of this figure.

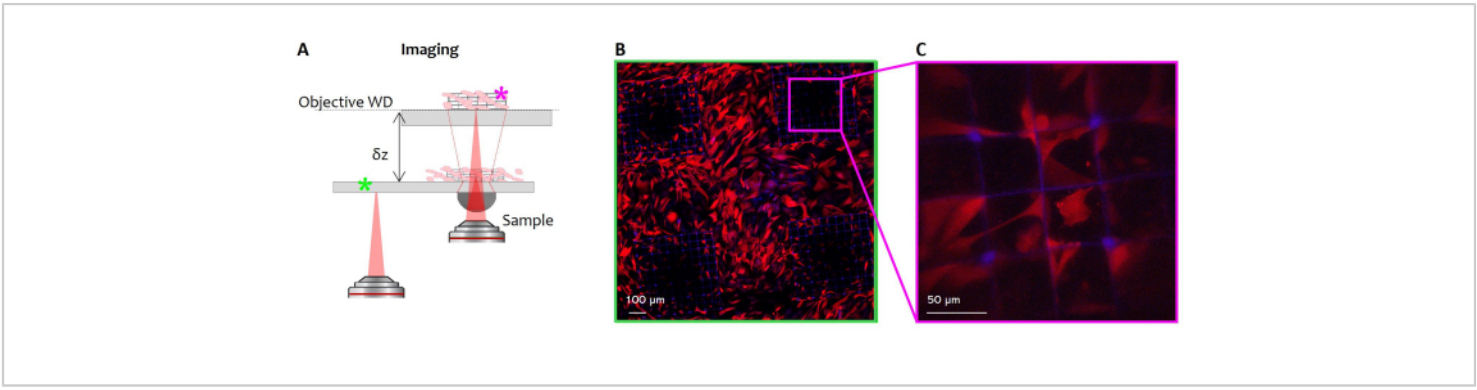

Figure 8: Potential application of the microstructured imaging window. On the left, a representative sketch illustrates the optical system constituted by the device coupled to an external microscope objective in a standard scanning system (**A**). This is the so-called virtual configuration used in this case for the imaging of living cell growth inside the micro-scaffold. Fluorescence fibroblasts (Red Fluorescence Protein (RFP) labeled) were seeded on the glass surface of the device, which bears the 3D microstructures. Confocal fluorescence images of cells have been taken at the glass coverslip focal plane (**B,** green hashtag), thus with the only use of the external objective, and through a single microlens at its focal plane (**A,** violet hashtag). Cell nuclei are visible in blue (Hoechst staining), and cytoskeleton in red (RFP). Scale bars: (**B**) - 100 µm; (**C**) - 50 µm. Please click here to view a larger version of this figure.

Discussion

To ensure accurate imaging of the desired area[3,6] in the micro-structured window, it is mandatory to have a precise alignment of the two structures (micro-scaffold and micro-lenses). This poses the main challenge of the proposed protocol as the high resolution of 2PP is closely related to a limitation in the fabrication depth[3,6]. Flipping the sample during fabrication to sequentially expose both surfaces to the laser beam may be an option, but it complicates re-alignment and is time-consuming[5]. This would also introduce difficulties in finding the same reference system and thus compromise the good alignment between micro-optical components and micro-scaffolds. Conducting the entire process continuously without unmounting the sample maintains a consistent reference system, thereby facilitating and guaranteeing accurate alignment of the structures. To do so, we use a long working distance objective (2.5 mm) that maintains a good resolution thanks to its high numerical aperture (step 1.1). This approach also significantly reduces fabrication time as it saves the alignment of the sample after flipping it[3]. Additionally, handling the samples poses another challenge due to their small size and fragility, making manipulation and precise alignment even more critical.

In 2PP processes, a wide investigation of the fabrication process is essential to establish key parameters such as the optimal laser wavelength, pulse width as well as laser powers and stage motions[9,10,11]. Therefore, a comprehensive characterization of the 2PP process, even considering different configurations of the experimental setup to first ensure highly stable, high-resolution 3D structures with cellular-scale detail for biological applications, has been performed[27,28,29,30]. Additionally, minimizing the surface

roughness of the implantable microlenses was crucial to obtaining high-quality micro-optics with the desired optical features, thereby reducing the immunological response to the implant[19,22,31]. Therefore, the process' challenge lies in adjusting parameters like power and pulse width based on experimental factors such as the refractive index and volume of the photosensitive material, environmental conditions (e.g., humidity and temperature), and laser efficiency. Extensive characterization was also required for UV exposure time and intensity to fully crosslink the entire volume of the microlenses, ensuring their stability. These settings must be tailored to the UV source, operating distance, and the specific volume of the element to be UV-polymerized.

A primary limitation of the 2PP process is its low throughput due to the extremely high resolution it offers. Given that, polymerized features are very small, from hundreds of nanometers to a few micrometers[9,26]. Therefore, fabrication times increase significantly when producing structures on the scale of hundreds of micrometers, which are relatively large by 2PP standards, especially if bulky structures. As a result, creating integrated devices with multiple structures of such big dimensions can take several hours. In this framework, the hybrid UV-2PP protocol proposed for microlenses manufacturing enhanced a 98% reduction in fabrication time of a single microlens compared to the 2PP of its entire volume. This allowed for increased precision in the 2PP scanning of the microlens' outer shell, reducing surface roughness while getting a microlens shell thick enough to ensure lens stability, all within a tolerable fabrication time. To further speed up the process, a parallelization approach will be proposed in the future to allow simultaneous writing of multiple structures[32]. This strategy would involve splitting the laser beam into multiple beams to create several focal points, enabling parallel fabrication and thereby greatly reducing overall production time.

Unlike the most common soft lithographic techniques, one of the key advantages of the 2PP is that it is a mask-less additive manufacturing approach that enables the fabrication of arbitrary structures within a volume of photosensitive material[11]. This capability allows the production of complex three-dimensional and porous structures with high customization potential. Moreover, based on the principle of non-linear absorption, the 2PP allows to reach resolution below the diffraction limit, which is unachievable by standard 3D printing techniques or fused deposition modeling (FDM) as an example[33]. This is particularly valuable for creating porous 3D scaffolds with cellular-scale features to support cellular growth, recruitment, and tissue integration.

The production of microstructured implantable devices with integrated optics by the process proposed here has the potential to significantly impact applications spanning mechanobiology, *in vitro* disease modeling, and tissue engineering (**Figure 7** and **Figure 8**). The presented protocol enables the fabrication of a high-quality technical device featuring microstructures that support tissue integration while simultaneously serving as *in vivo* imaging reference points. Additionally, those properly designed microlenses enhanced advanced non-linear imaging by correcting spherical aberrations caused by the tissue surrounding the implant[4]. The versatility of the process, in fact, allows us to adjust the design of the device like, for example, to create scaffolds and reference structures with a geometry optimized for specific applications, helping in both 3D reconstructions and correction of imaging aberrations in post-processing. Lastly, tailoring microlens design based on tissue refractive

indices enhances application-specific imaging, effectively creating an *in situ* optical lens within the device.

Disclosures

The authors declare no conflict of interest.

Acknowledgments

This research has received funding from the European Union under the Horizon 2020 research and innovation program (G.A. No. 964481-IN2SIGHT).

References

1. Sadakane, O. et al. *In vivo* two-photon imaging of dendritic spines in marmoset neocortex. *eNeuro.* **2** (4), 1-10 (2015).
2. Prunier, C., Chen, N., Ritsma, L., Vrisekoop, N. Procedures and applications of long-term intravital microscopy. *Methods.* **128**, 52-64 (2017).
3. Marini, M. et al. Microlenses fabricated by two-photon laser polymerization for cell imaging with non-linear excitation microscopy. *Adv Funct Mater.* **33** (39), 202213926 (2023).
4. Kariman, B. S. et al. High dioptric power micro-lens fabricated by two-photon polymerization. *Opt Express.* **32** (27), 48114-48131 (2024).
5. Conci, C. et al. Advanced optical materials. *Adv Opt Mater.* **10** (7), e2101103 (2022).
6. Conci, C. et al. *In vivo* label-free tissue histology through a microstructured imaging window. *APL Bioeng.* **8** (1), 016107 (2024).
7. Dondossola, E. et al. Examination of the foreign body response to biomaterials by non-linear intravital microscopy. *Nat Biomed Eng.* **1** (1), 1-10 (2017).
8. Lee, K. S., Kim, R. H., Yang, D. Y., Park, S. H. Advances in 3D nano/microfabrication using two-photon initiated polymerization. *Prog Polym Sci.* **33** (6), 631-681 (2008).
9. LaFratta, C. N. et al. Multiphoton fabrication. *Angew Chem Int Ed.* **46** (33), 6238-6258 (2007).
10. Malinauskas, M. et al. Ultrafast laser nanostructuring of photopolymers: A decade of advances. *Phys Rep.* **533** (1), 1-31 (2013).
11. Zyla, G., Farsari, M. Frontiers of laser-based 3D printing: A perspective on multi-photon lithography. *J Laser Micro/ Nanoeng.* **19** (1), 1-12 (2024).
12. Eltom, A., Zhong, G., Muhammad, A. Scaffold techniques and designs in tissue engineering functions and purposes: A review. *Adv Mater Sci. Eng.* **2019**, 3429527 (2019).
13. Yang, X. et al. Additive manufacturing of polymer-derived ceramics. *Adv Powder Metall Part Mater.* **351** (6268), 716-725 (2020).
14. Cai, Y. Z. et al. Novel biodegradable three-dimensional macroporous scaffold using aligned electrospun nanofibrous yarns for bone tissue engineering. *J Biomed Mater Res. A.* **100 A** (5), 1187-1194 (2012).
15. Nandakumar, A. et al. A fast process for imprinting micro and nanopatterns on electrospun fiber meshes at physiological temperatures. *Small.* **9** (20), 3405-3409 (2013).
16. Yuan, W. et al. Fabrication of microlens array and its application: A review. *Chin J Mech Eng.* **31** (1), 20 (2018).
17. Cai, S. et al. Microlenses arrays: Fabrication, materials, and applications. *Microsc Res Tech.* **84** (11), 2784-2806 (2021).

18. Vaezi, M. et al. A review on 3D micro-additive manufacturing technologies. *Int J Adv Manuf Technol.* **67** (5-8), 1721-1754 (2013).
19. Guo, R. et al. Microlens fabrication by means of femtosecond two-photon photopolymerization. *Opt Express.* **14** (2), 810 (2006).
20. Malinauskas, M. et al. A femtosecond laser-induced two-photon photopolymerization technique for structuring microlenses. *J Opt.* **12** (3), 035204 (2010).
21. Siegle, L. et al. Complex aspherical singlet and doublet micro-optics by grayscale 3D printing. *Opt Express.* **31** (3), 4179 (2023).
22. Gissibl, T. et al. Two-photon direct laser writing of ultracompact multi-lens objectives. *Nat Photonics.* **10** (8), 554-560 (2016).
23. Thiele, S. et al. 3D printed stacked diffractive microlenses. *Opt Express.* **27** (24), 35621 (2019).
24. Balli, F. et al. A hybrid achromatic metalens. *Nat Commun.* **11** (1), 17646 (2020).
25. Gonzalez-Hernandez, D. et al. Laser 3D printing of inorganic free-form micro-optics. *Photonics.* **8** (12), 577 (2021).
26. Ovsianikov, A. et al. Ultra-low shrinkage hybrid photosensitive material for two-photon polymerization microfabrication. *ACS Nano.* **2** (11), 2257-2262 (2008).
27. Madden, L. R. et al. Proangiogenic scaffolds as functional templates for cardiac tissue engineering. *Proc Natl Acad Sci USA.* **107** (34), 15211-15216 (2010).
28. Raimondi, M. T. et al. Three-dimensional structural niches engineered via two-photon laser polymerization promote stem cell homing. *Acta Biomater.* **9** (1), 4579-4584 (2013).
29. Guillaume, O. et al. Hybrid spheroid microscaffolds as modular tissue units to build macro-tissue assemblies for tissue engineering. *Acta Biomater.* **165**, 72-85 (2023).
30. Ovsianikov, A., Mironov, V., Stampf, J., Liska, R. Engineering 3D cell-culture matrices: Multi-photon processing technologies for biological and tissue engineering applications. *Expert Rev Med Devices.* **9** (6), 613-633 (2012).
31. Noskovicova, N., Hinz, B., Pakshir, P. Implant fibrosis and the underappreciated role of myofibroblasts in the foreign body reaction. *Cells.* **10** (7), 1794 (2021).
32. Zandrini, T. et al. Multi-foci laser microfabrication of 3D polymeric scaffolds for stem cell expansion in regenerative medicine. *Sci Rep.* **9** (1), 1-9 (2019).
33. Rey, F. et al. Advances in tissue engineering and innovative fabrication techniques for 3D structures: Translational applications in neurodegenerative diseases. *Cells.* **9** (7), 1636 (2020).